Resonant-Cavity Light-Emitting Diodes: a review

Roel G. Baets, Danaë Delbeke, Ronny Bockstaele and Peter Bienstman
Ghent University, Department of Information Technology (INTEC)
Sint-Pietersnieuwstraat,41, B-9000 Gent, Belgium
photonics.intec.rug.ac.be

ABSTRACT

An overview of planar resonant-cavity light-emitting diodes is presented. Letting spontaneous emission happen in a planar cavity will in the first place affect the extraction efficiency. The internal intensity distribution is not longer isotropic due to interference effects (or density of states effects). The basics of dipole emission in planar cavities will be shortly reviewed using a classical approach valid in the so called weak-coupling regime. The total emission enhancement or Purcell factor, although small in planar cavities, will be explained. The design of a GaAs/AlGaAs RCLED is discussed. We review the state-of-the-art devices in different semiconductor material systems and at different wavelengths. Some advanced techniques based on gratings or photonic crystals to improve the efficiency of these devices are discussed. RCLEDs are not the only candidates that can be used as high-efficiency light sources in communication and non-communication applications. They compete with other high-efficiency LEDs and with VCSELs. The future prospects of RCLEDs are discussed in view of this competition.

Keywords: resonant-cavity; micro-cavity; light-emitting diode; semiconductor

1. INTRODUCTION

High radiance, modulation capabilities, spectral purity and efficiency are no longer exclusively attributed to lasers. Since the invention and first demonstration[1] in 1992 of the Resonant-Cavity LED (RCLED) which uses photon quantisation in microcavities to enhance spontaneous emission properties, directionality, intensity and purity can as well denote key performance characteristics of LEDs. These assets make RCLEDs particularly suited for optical communication applications, more specifically data communication via Plastic Optical Fiber (POF) and infrared wireless communication.

The internal isotropic spontaneous emission field distribution represents the main limitation to acquire high efficiencies in standard LEDs. Due to the large refractive index of the light emitting medium, the efficiently generated photons can only be extracted when they impinge on the interface with an incidence angle smaller than the critical angle defined by total internal reflection (Snell's law). For a semiconductor LED (e.g. $n_1 \approx 3.5$) in air ($n_2=1$), the critical angle $\theta_c = \text{asin}(n_2/n_1) \approx 16^o$. Consequently, only a fraction ≈2 % of the isotropically emitted photons can be extracted (single-side extraction). Several solutions have been presented that successfully outsmart Snell's law. Geometrical issues like slanted interfaces, surface roughening, etc. enhance the extraction probability of the isotropically emitted photons. RLCEDs, on the other hand, cancel the intrinsically isotropic emission profile. Conceptually, a RCLED consists of a high reflective mirror, a cavity with a thickness in the order of the wavelength including the active layer with several quantum wells for light generation, and a semi-transparent mirror for light extraction. The mirrors make up a (Fabry-Perot) resonator in which constructive and destructive interferences dictate the possible emission directions. The latter corresponds with resonant modes. With an appropriate cavity design, the preferential propagation direction of the photons can thus be forced from total internal reflection regime towards the extraction cone, benefitting to the extraction efficiency. Together with this increase of directivity and/or efficiency due to a redistribution of the photons, the spontaneous emission rate will be enhanced due to the Purcell-effect. However, because of the planar geometry and the rather small reflectivity coefficients of the cavity mirror(s) in practical applications, the Purcell-factor is close to one, resulting in a negligible spontaneous emission rate enhancement (see section 2.2).

Spontaneous emission in a layered medium is summarised in section 2. For more details, the reader is referred to [2,3]. Application of this theory is illustrated in section 3 by the design of a GaAs/AlGaAs RCLED. Section 4 gives an idea of the state of the art of the RCLED in different material systems. Further improvement by advanced techniques is discussed in section 5.

Light-Emitting Diodes: Research, Manufacturing, and Applications VII,
E. Fred Schubert, H. Walter Yao, Kurt J. Linden, Daniel J. McGraw, Editors,
Proceedings of SPIE Vol. 4996 (2003) © 2003 SPIE · 0277-786X/03/$15.00

2. SPONTANEOUS EMISSION IN A LAYERED MEDIUM

2.1 Non-isotropic emission profile of dipole in layered medium

In a Resonant-Cavity (RC) or Micro-Cavity (MC) LED, spontaneous emission happens in a multi-layer Fabry-Perot resonator. Interference effects alter the internal angular power distribution (Fig. 1). Directions of constructive and destructive interference alternate, corresponding respectively with directions in which light emission is enhanced and suppressed. In the so-called "weak coupling" regime the spontaneous emission of electron/hole pairs is adequately represented by an electric dipole. The normalized monochromatic electromagnetic field from the dipole can be Fourier transformed with respect to x and y in a set of plane waves with an amplitude A expressed as a density per unit solid angle. The $\mathbf{k}_{//}$ Fourier spectrum contains arbitrarily large wave vectors $\mathbf{k}_x$ and $\mathbf{k}_y$ spanning propagative ($|\mathbf{k}_{//}| \le n_s k_0$) and evanescent contributions ($|\mathbf{k}_{//}| > n_s k_0$), with n_s the refractive index of the source layer, $k_0 = 2\pi/\lambda_0$ and λ_0 the vacuum wavelength and $\mathbf{k}_{//} = \mathbf{k}_x + \mathbf{k}_y$. The z-component of $\mathbf{k}$, k_z, can be expressed as a function of $k_{//}$:

$$k_z = \pm\sqrt{n_s^2 k_0^2 - k_x^2 - k_y^2} = \pm\sqrt{n_s^2 k_0^2 - k_{//}^2} \qquad \text{(eq.1)}$$

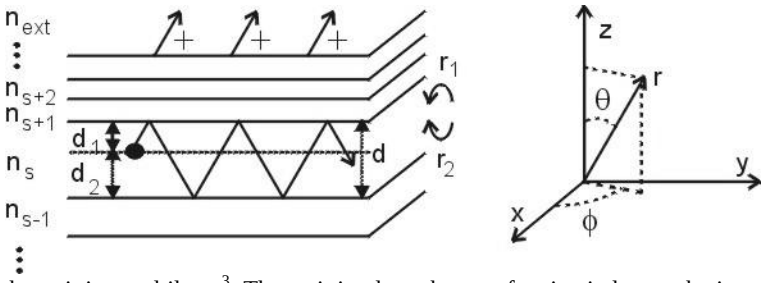

Figure 1: Sketch of a light-emitting multilayer[3]. The emitting layer has a refractive index n_s, the intermediate layers $n_{s\pm1}$, $n_{s\pm2}$,… the half infinite surrounding media n_{ext}. d is the thickness of the emitting layer. The dipole is located at a distance d_1 from the interface with the first layer of the upper mirror; at a distance d_2 from the interface with the first layer of the bottom mirror. The upper mirror has a reflection coefficient r_1; the bottom mirror a reflection coefficient r_2. Interference takes place when the radiation is reflected back and forth between the two interfaces of the layer. The emission angle θ and ϕ are defined in the *xyz*-coordinate system.

A plane wave component **A** of the field resulting from an electric dipole has its electric field in the plane of the dipole moment and the wavevector **k**, vanishing sinusoidally for emission in the direction of the dipole moment. An arbitrary linear polarisation can be decomposed in TE (Transverse Electric or s: the plane wave has its E-field in the (x-y)-plane and orthogonal to k) and TM (transverse magnetic or p: has its H-field transverse to the plane of incidence). The *vectorial* electromagnetic problem is then transformed in independent simple *scalar* problems[3]. Due to the polarisation maintaining reflection and refraction of TE and TM-waves upon a planar interface, the electromagnetic analysis of plane wave propagation in a layered medium is decomposed in two uncoupled scalar systems. The emitted field $E^{pol}(\theta)$ and emitted intensity $I^{pol}(\theta)$, with θ the internal emission angle, caused by the source's downwards and upwards propagating plane wave component $A_{\downarrow}^{pol}$ and $A_{\uparrow}^{pol}$ ($pol=s,p$) can be calculated by letting the plane propagative and evanescent waves propagate in the multilayer. The different contributions in the outside medium (Fig. 1) give rise to a field distribution, a power distribution and an extraction efficiency given by:

$$E^{pol}(\theta) = \left[A_{\uparrow}^{pol} + A_{\downarrow}^{pol} r_2 \exp(-j2\phi_2)\right] t_1 \exp(-j\phi_1).\left[1 + r_1 r_2 \exp(-j2\phi) + r_1^2 r_2^2 \exp(-j4\phi) + \ldots\right] \qquad \text{(eq.2)}$$

$$I^{pol}(\theta) = T_1 \left|E^{pol}(\theta)\right|^2 = T_1 \frac{\left|A_{\uparrow}^{pol} + A_{\downarrow}^{pol} |r_2| \exp(-j2\phi_{2eff})\right|^2}{\left|1 - |r_1 r_2| \exp(-j2\phi_{eff})\right|^2} \qquad \text{(eq.3)}$$

$$\eta_{extr} = \frac{2\pi \int_0^{\theta_C} I^{pol}(\theta) \sin\theta d\theta}{2\pi \int_0^{\pi} I^{pol}(\theta) \sin\theta d\theta} \qquad \text{(eq.4)}$$

with $|r_1 r_2|<1$, r_1, r_2 the upwards and downwards amplitude reflection coefficients, T_1 the upwards power transmission coefficient, $\phi_i = k_0 n_s d_i \cos(\theta)$, i=1,2, $\phi = \phi_1 + \phi_2$ and $2\phi - \arg(r_1) - \arg(r_2) = 2\phi_{eff}(\theta,\lambda)$ and $2\phi_i - \arg(r_i) = 2\phi_{i,eff}(\theta,\lambda)$ and d_1 and d_2 the distances of the dipole from the interfaces of respectively the first layer of the upper mirror and the first layer of the bottom mirror. r_1, r_2 and T_1 are polarisation dependent and can be calculated using the transfer matrix method. The numerator is called the *standing wave factor* $\zeta(\phi_{2\ eff})$ and expresses the dependence of the emitted intensity on the position of the source: emission is high in a particular direction if the source is located in an antinode of the standing wave field. The denominator does not dependent on the position of the source, but depends strongly on λ and θ. The inverse of the denominator is called the *cavity enhancement factor* or *Airy factor* $\Gamma(\phi_{eff})$. The Airy function is periodic with a period π in ϕ_{eff} and at a maximum, the cavity is said to be *resonant*. These maxima define the *resonant modes* and obey the phase condition $2\phi - \arg(r_1) - \arg(r_2) = 2\phi_{eff}(\theta,\lambda) = 2m\pi$, with m a positive or negative integer. These resonances account both for Fabry-Perot ($\theta < \theta_c$) and guided modes ($\theta > \theta_c$). The resonator is "perfect" when $|r_1 r_2|=1$. The resonant mode will not be damped when the excitation is switched off in a perfect resonator. This happens when there are no extraction or absorption losses. If $|r_1 r_2|<1$, the optical mode densitiy is not longer a Dirac distribution, the resonant peaks $\delta\phi_{\text{eff}}$ caused by the Airy factor $\Gamma(\phi_{eff})$ have a finite width. The FWHM is inversely proportional to the finesse F (Fig. 2(a)):

$$F \equiv \frac{\Delta\phi_{eff}}{\delta\phi_{eff}} = \frac{\pi}{\delta\phi_{eff}} \qquad \text{(eq.5)}$$

with $\Delta\phi_{eff}$ the separation between two adjacent resonances. The *cavity order* m_c is defined as the normalized cavity length:

$$m_c \equiv \frac{d}{\lambda_0 / 2n_s} \qquad \text{(eq.6)}$$

The phase of the reflection coefficients r_1 and r_2 of a multilayer depends on the angle of incidence. For the extractable Fabry-Perot, the phase changes approximately in a linear way with the angle of incidence. An effective penetration depth can thus be defined as the depth measured from the interface, where an ideal mirror interface should be positioned to give rise to the same variation of the phase. This penetration depth needs to be added to the cavity thickness d to define the effective cavity thickness d_{eff} and with this the effective cavity order $m_{c\ eff}$:

$$d_{eff} = d + d_{pen} = d + \frac{\lambda_0}{2n_s} \frac{-\partial(\arg(r_1) + \arg(r_2))}{\partial \cos\theta} \frac{1}{2\pi}$$
$$m_{ceff} = \frac{d_{eff}}{\lambda_0 / 2n_s} \qquad \text{(eq.7)}$$

The cavity order $m_{c\ eff}$ is a measure for the number of resonant modes in the cavity: considering the phase condition $m_{ceff}\cos\theta = m$, it is clear that the number of resonances is limited to about $\lfloor m_{c\ eff} \rfloor$ (with $\lfloor \_ \rfloor$ the largest integer smaller than the argument). When the resonances of the cavity have a high F, η_{extr} can be estimated: the Airy function can be approximated by a Dirac distribution for which η_{extr} is translated to a ratio of discrete sums. The numerator accounts for the Fabry-Perot modes and the denominator for all modes, both Fabry-Perot (giving rise to propagative waves outside the cavity) and guided (giving rise to evanescent waves outside the cavity) modes. With a single mode in the extraction cone, and excitation of only the even modes (determined by the position of the active layer), η_{extr} is given by:

$$\eta_{extr} \cong \frac{\sum_{i,\theta<\theta_C} \zeta_i}{\sum_i \zeta_i} = 1/\left(\lfloor m_{ceff} \rfloor / 2\right) \qquad \text{(eq.8)}$$

(eq.8) shows that the extraction efficiency depends on the effective cavity order and thus the penetration depth of the mirror. Typically, the penetration depth is positive, resulting in an increase of $m_{c\ eff}$ and a decrease of η_{extr}. A novel design -the RC2LED- realizes a negative penetration depth using a non-periodic high index-contrast mirror[4]. This

negative penetration depth creates extra resonances in the extraction cone, which boosts the extraction efficiency 50 to 100% higher than conventional RCLEDs to a specific NA.

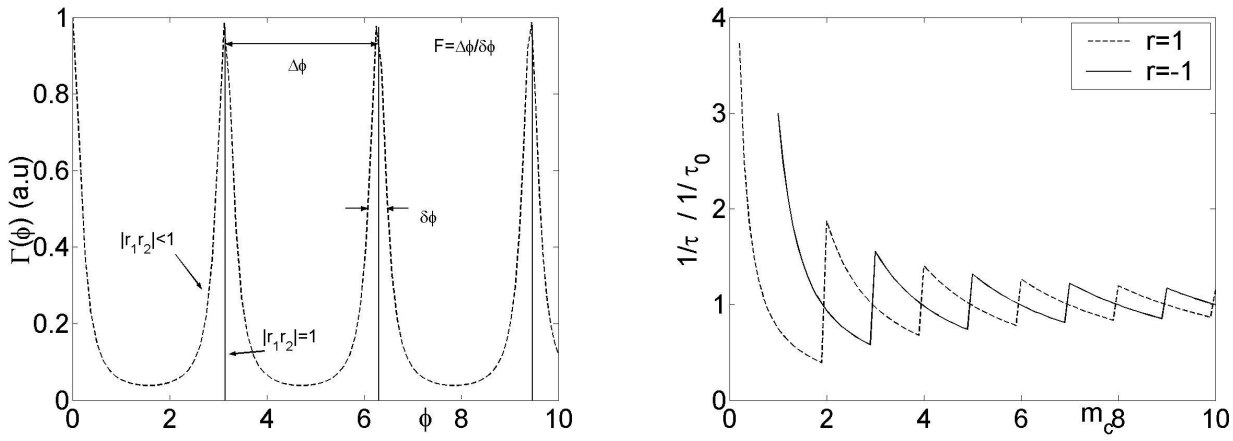

Figure 2: (a) Cavity enhancement factor or Airy Factor in function of ϕ, with graphical definition of *F;* (b) Modification of spontaneous emission rate or Purcell effect[3].

2.2 Purcell effect

Letting spontaneous emission happen in a cavity will influence the total emitted power. For a given density of dipoles per unit volume, a change in the total emitted power can, in case a dipole represents radiative electron-hole recombination, only be associated with a change in recombination rate and hence lifetime:

$$\frac{\frac{1}{\tau}}{\frac{1}{\tau_0}} = \frac{\text{emitted dipole power in cavity}}{\text{emitted dipole power in bulk}} \qquad \text{(eq.9)}$$

where τ and τ_0 are the respective lifetimes with and without cavity. The change of carrier lifetime due to the presence of a cavity is known as the Purcell effect. The Purcell-factor expresses this carrier lifetime change and has been derived by Purcell as $(3Q/4\pi^2)(\lambda^3/V)$. It is defined for 3-D optical cavities of volume V and mode quality factor $Q=\lambda/\delta\lambda$ with $\delta\lambda$ the narrow emission linewidth around λ.

An analytical expression for the SE enhancement has been derived for the case of a horizontal dipole in the middle of a cavity with perfect mirrors[5]. For $r=+1$ there are $\lfloor m_{c\ eff} \rfloor = \lfloor m_c \rfloor + 1$ modes but only $\lfloor m_c/2+1 \rfloor$ are excited. The others are not excited because the dipole is located at a zero of the mode profile. For r=-1 there are $\lfloor m_{c\ eff} \rfloor = \lfloor m_c \rfloor$ modes, $\lfloor (m_c+1)/2 \rfloor$ of which are excited The calculated decay rate enhancement is presented in Fig. 2(b). One can see that apart from the singular $1/m_c$ behavior for small m_c in the $r=+1$ case, the maximum SE enhancement is 3 and is obtained in a half-wavelength thick cavity with $r=-1$ (perfect metallic mirrors). For thick cavities the Purcell effect converges to 1. In other words, thick cavities with many modes have a similar impact on the dipole as uniform space with a continuum of modes. For real metals, the phase shift lies in between these extreme cases, and can give rise to an intermediate Purcell-factor. A 4.4-fold enhancement is experimentally shown for a GaAs cavity with two Cr/Ag mirrors[6]. Bragg mirrors modify only weakly the spontaneous emission of a semiconductor emitter (typically 1.2 (GaAs/AlGaAs)-1.4 ($GaAs/AlO_x$)[5]), due to the large leaks they present at the oblique incidences and due to the larger penetration depth.

The Purcell effect can be substantially larger in 3-D cavities than in planar cavities. A strong enhancement of the spontaneous emission rate has been observed for self-assembled InAs/GaAs quantum boxes inserted in GaAs-based pillar microcavities (x5) and microdisks (x15) using time-resolved as well as c.w. photoluminescence experiments, and in spite of various detrimental averaging effects compared to the ideal case[7].

3. ILLUSTRATIVE EXAMPLE: NON-SYMMETRIC GAAS/ALGAAS RCLED

The design of a GaAs/AlGaAs RCLED emitting at 980 nm will be discussed. This textbook example will show the importance of mirror choice, cavity tuning, etc. in view of its performance. Some design rules come herewith.

3.1 Mirrors

The efficiency of the RCLED depends strongly on both amplitude and phase of the reflection coefficient of the cavity mirrors. Fig. 3 generically shows the amplitude and penetration depth of different mirrors as a function of the angle of incidence for TE and TM polarization: a semiconductor/metal interface, a semiconductor/air interface and a DBR mirror. A DBR mirror consists of a periodic quarter-wave stack of alternating high and low index material.

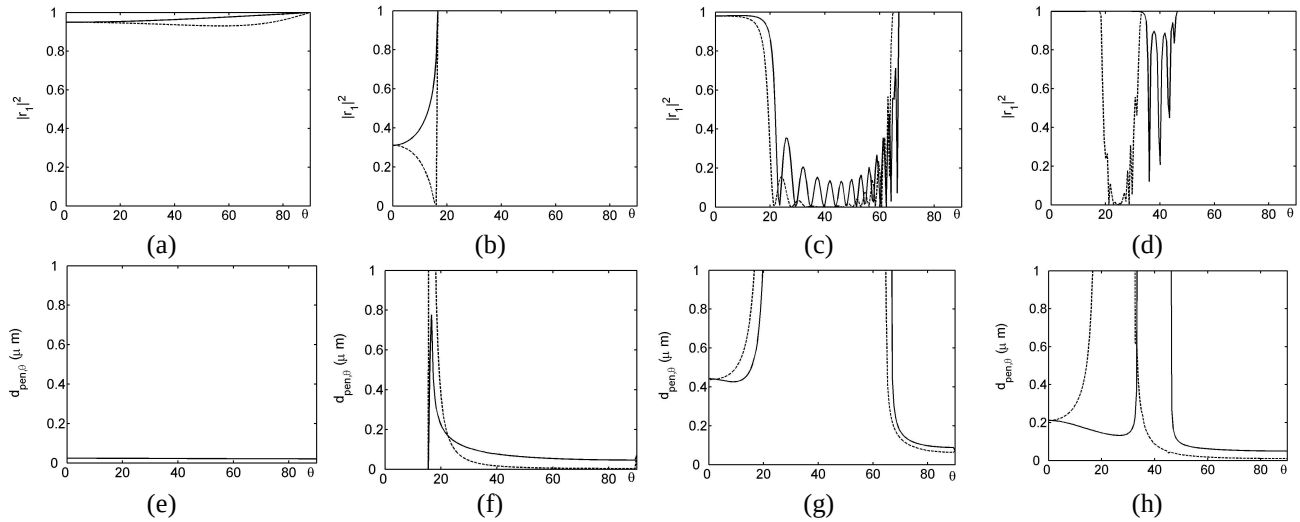

Figure 3: Reflectivity and penetration depth as a function of the incident angle ($\lambda=\lambda_{DBR}$=980nm) Full line: TE-polarization; dashed line: TM-polarization. (a-e) GaAs/Au interface; (b-f) GaAs/Air interface; (c-g) GaAs/(AlAs-GaAs DBR)/GaAs interface (N=30)(d-h) GaAs/(AlOx-GaAs DBR)/GaAs interface (N=10)[3].

(eq.8) shows that the penetration depth has to be minimal to enhance the extraction efficiency. This accounts both for the back mirror or high reflective mirror and outcoupling mirror or semi-transparent mirror. For the outcoupling mirror, absorption losses have to be low.

Fig.3 shows that the penetration depth is minimal when a metallic mirror is used. However, due to its high absorption losses, a metallic mirror is preferably not used as an outcoupling mirror. As back mirror, the metal is deposited on the semiconductor. The component is bottom-emitting. The metal can both serve as mirror and electrical contact.

Comparison of Fig.3 (g) and (h) shows that the penetration depth of a DBR mirror decreases with increasing refractive index-contrast. For $\lambda=\lambda_{DBR}$ and for a large number N of DBR pairs, an approximate expression for the penetration depth can be deduced:

$$d_{pen} \approx \frac{n_s^2}{2}\left(\frac{1}{n_H^2}+\frac{1}{n_L^2}\right)\frac{\lambda_{DBR}}{4n_s^2}\frac{n_H n_L}{n_H - n_L} \qquad \text{(eq.10)}$$

with n_H, n_L respectively the highest and lowest refractive index of the DBR stack. (eq.10) holds for a large number N of DBR pairs. When the number of DBR pairs is decreased, the penetration depth will be lower. The choice of the number of DBR pairs tunes as well the amplitude of the reflection coefficient. Both requirements of the semi-transparent outcoupling mirror (moderate reflectivities and low absorption losses) and back mirror (high reflectivity) can thus be met when a transparent set of materials with high refractive index contrast can be found. On the other hand, the angular response of a DBR (Fig. 3) gives evidence of a high reflectivity around

$\theta=0^o$: $\Delta\cos\theta=2/\pi\ \Delta n/n_s$ but vanishes for larger θ. Reflection rises again when TIR inside the DBR is met. The part with low reflectivity gives rise to a continuum of optical modes, called the DBR-leaky modes. This is comparable with emission in bulk. These modes and the guided modes in the TIR regime are lost.

Fig. 4(a) shows the simulated extraction efficiency (η_{extr}) of a bottom-emitting GaAs/AlGaAs RCLED with λ-cavity (active layer consists of 3 InGaAs QWs) emitting at 980nm with intrinsic spectral width = 20nm (Gaussian spectrum is assumed). Fig. 4(b) shows the downwards internal emission profile for different numbers of DBR-pairs. The Fabry-Perot mode ($\theta<\theta_c$), leaky modes ($\theta_c<\theta<\theta^{TIR}_{DBR}$) and guided mode can be distinguished. The farfield pattern can be deduced when considering the angles smaller than the critical angle for TIR ($\theta_c\approx16^o$). The cavity is formed by a Au back mirror, deposited on top of the epitaxy layers. The outcoupling mirror is a DBR. η_{extr} is given as a function of the number of DBR-pairs and the top spacer thickness. The top spacer is the GaAs epitaxy layer above the active layer on which the Au mirror is deposited. The active layer is placed at an antinode of the extractable Fabry-Perot mode to maximise the standing wave factor $\zeta(\phi_{2\ eff})$. The importance of a moderate reflectivity to obtain a high η_{extr} is clear. η_{extr} is maximal (≈16%) for 5 DBR pairs (R=0.51). The reason is triple: Considering a monochromatic source in a lossless cavity, η_{extr} is proportional to the ratio of the area below the Airy function within the extraction cone to the total spanned surface. It is thus clear that the finesse of the Fabry-Perot mode has an optimal value, such that the peak resides well in the extraction cone, and above which value η_{extr} increases only marginally (see e.g. Fig.4(b)). Secondly, practical cavities have absorption losses. A moderate R prevents a large number of round-trips in the cavity, minimizing the absorption losses. Finally, due to the nonzero natural linewidth of the dipole source (the emitting material intrinsic spectrum), improving extraction efficiency at some wavelengths occurs at the expense of other wavelengths, which can cause a decrease of the spectrally integrated efficiency. When Q of the Fabry-Perot mode is larger than the intrinsic Q, it is of no use to enlarge the finesse of the cavity.

3.2 Cavity tuning

Fig. 4(a) demonstrates as well η_{extr} as a function of the cavity thickness. Fig. 4(c) shows the downwards internal emission profile for different cavity thicknesses. The highest η_{extr} is obtained when the cavity is detuned towards longer wavelengths relative to the QW emission wavelength ($d=125$nm). In this case, the Fabry-Perot enhancement will be located optimally in the extraction cone and η_{extr} is maximised as it is proportional to the ratio of the area below the Airy function within the extraction cone to the total spanned surface. The detuning will influence the external emission profile strongly: the "rabbit-ears" in the emission pattern are an unavoidable property of highly efficient RCLEDs. This results in different design parameters for devices with an overall high efficiency and devices with a high efficiency towards a limited NA around the surface normal direction needed in optical fiber communication applications. A deviation of the cavity thickness in the order of $\lambda/10$ from the optimal value can result in a reduction of the efficiency by a factor 3. The performance of the RCLED is in direct relation with the precision of the growth of the cavity thickness.

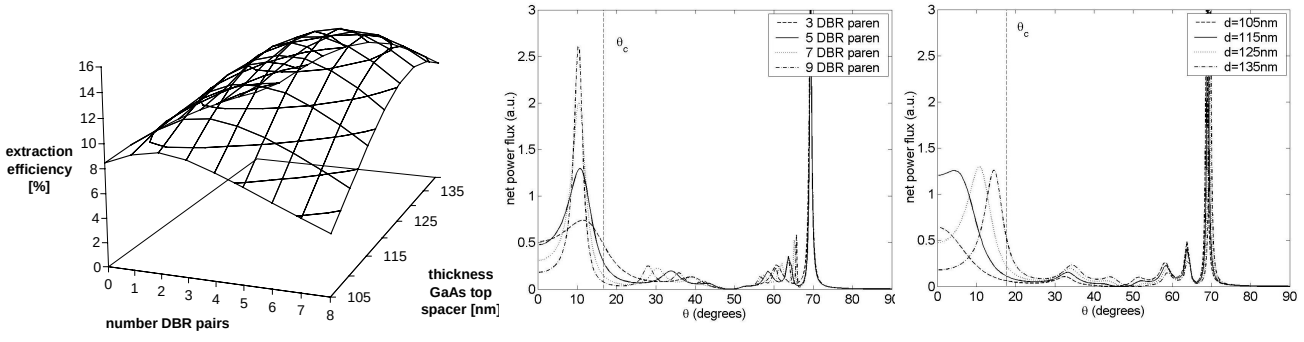

(a) (b) (c)

Figure 4: (a) extraction efficiency of GaAs/AlGaAs RCLED emitting at 980 nm and intrinsic spectral width 20nm, in function of the thickness of the top spacer and of the number of DBR pairs; (b) net power flux or internal emission distribution per unit solid angle as a function of the number of DBR pairs (d=125nm); (c) net power flux or internal emission distribution per unit solid angle as a

function of the top spacer thickness *d* (5 DBR pairs). The top spacer is the GaAs layer on top of the active layer. The farfield pattern can be deduced from these graphs by considering the angles smaller than θ_c.

An extractable Fabry-Perot mode is obtained when the thickness of the cavity is a multiple of half the wavelength. The described RCLED has a cavity with a thickness = λ. When the cavity thickness is increased with a multiple of $\lambda/2$, the amount of resonances will increase. The ratio of the area below the Airy function within the extraction cone to the total spanned surface under the emission profile will decrease as well as η_{extr} (see also above). Ideally, the total optical power is emitted in a single extractable Fabry-Perot mode, using a $\lambda/2$-cavity. However, λ-cavities are in generally used in practical applications for several reasons. In case the cavity is set up by metallic mirror(s), a $\lambda/2$-cavity implies that the distance of the active layer to the metal is very small and can result in considerable losses due to nonradiative energy transfer from the dipole to the absorptive metal. For a perfect mirror with phase shift π the distance is maximally $\lambda/4$ (e.g. about 70 nm for a GaAs RCLED emitting at 980 nm). For realistic metallic mirrors, with a phase shift different from π, this distance is even further reduced by some tens of nanometers (a reduction of about 45 nm for a GaAs RCLED emitting at 980 nm with Au-mirror). Moreover, from a technological point of view, a λ-cavity is preferable to its thinner counterpart, and will in general be used in practical devices both when metallic mirrors or dielectric mirrors are used. A metallic mirror requires a heavily doped contact layer to ensure good electrical contact. Experiments evidenced that minimal thicknesses of several tens of nanometer (50 nm for a GaAs RCLED emitting at 980 nm with Au-mirror) are needed for the contact layer. As this contact layer (heavily doped GaAs) extends to a distance of some 20nm from the active layer, there is not much space left for band gap engineering to optimize the device. Multiple QW layers sandwiched in a carrier confinement structure (like Graded Refractive Index (GRIN) confinement structures optimizing carrier caption) typically have a total thickness of about 120 nm. When dielectric mirrors are used, a sideways current supply is needed to pump the device. In this case again, a minimal thickness can be needed. To achieve proper carrier injection and low series resistance, extra layers can be added in the cavity.

3.3 Saturation of the optical power

At high pump levels, the optical power emitted by the device can saturate. This results from several effects. At low current densities, a broadening of the intrinsic spontaneous emission profile in function of the current density is observed. This carrier density dependence of the spectral width is called band filling. The overlap between the cavity resonance and the intrinsic spectrum decreases, and thus the extraction efficiency too. Secondly, at higher current levels, thermal effects become important and let decrease the efficiency faster. Non-radiative recombination and ohmic heating by the series resistance results in a temperature increase of the active region. The temperature increase has two consequences. Firstly, the internal quantum efficiency decreases. Secondly, the cavity resonance wavelength (mainly due to the temperature dependency of the refractive index, and little due to the thermal expansion of the material) and the intrinsic emission wavelength (due to the decreasing gap energy of semiconductors with increasing temperature) will shift at different rates towards longer wavelengths. The shift of the cavity resonance is much smaller than the shift of the peak wavelength emitted from the active semiconductor material. This results in a temperature dependent overlap between the intrinsic emission spectrum and the cavity enhancement, and a decreasing extraction efficiency when increasing current[8]. At high current levels, the optical power does not increase anymore and saturates to value of several $\mu W/\mu m^2$ depending on the thermal resistance of the ambient media.

3.4 Photon recycling

Light emitted by the active region can be reabsorbed by the active region. The generated carriers can then recombine again, releasing a new photon. This effect is called photon recycling and increases the internal efficiency η_{int} and thus the overall external efficiency η_{ext} of the device, as an electron will have a higher probability to produce a photon that escapes from the cavity. This effect occurs in devices with a thick active region. QW based devices have in general no influence of this reabsorption effect. However, in microcavities, a part of the generated light is emitted in the laterally propagating guided modes, which have an increased overlap with the QWs. The increase of η_{int} will thus depend on two factors: the number of photons emitted into the guided mode and the characteristic absorption length of the guided mode. The characteristic absorption length is a function of the absorption coefficient of the active layer (which depends on the carrier density in the active layer) and the overlap between the internal field profile and the active layer. The guided mode is not necessarily concentrated around the active layer: the field profile can be concentrated in the DBR, resulting in a rather small overlap factor. Typically, the absorption length is 100μm. Consequently, the recycling effect

is present in large diameter devices and negligible (or even absent) in small diameter devices. Fig. 5(a) shows the calculated increase of η_{int} in case of full lateral reabsorption (i.e. device diameter much larger than reabsorption length) and assuming an internal quantum efficiency η_{int} =90%. The recycling increases as function of the number of DBR pairs, for which the profile around is more concentrated around the active layer, increasing the overlap. The influence of a variation of the thickness of the top spacer of the cavity is less pronounced. In large devices, the recycling effect results in a 1.4 times enhancement of the overall efficiency[10].

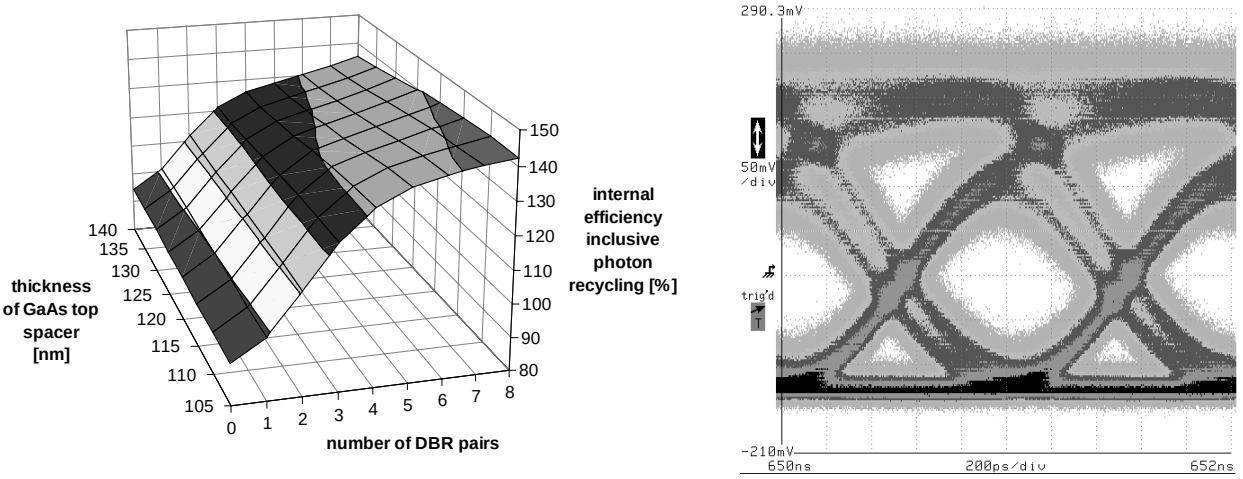

(a) (b)

Figure 5: (a) Efficiency increase due to recycling as a function of top spacer thickness and number of GaAs/AlAs DBR pairs of GaAs λ-cavity emitting at 980 nm [3]. (b) Measured eye-diagram of voltage-driven 980-nm RCLED at 1Gbit/s (diameter = 30 μm)[9].

3.5 Modulation bandwidth

The modulation bandwidth is directly related to the radiative recombination speed. The radiative recombination speed is found after averaging the recombination lifetime of an electron-hole pair in the semiconductor over all available energy levels of the electrons and holes in the active region. The radiative recombination lifetime alteration in a micro-cavity, known as the Purcell effect, was discussed in section 2.2. The micro-cavity which alters the optical mode density and the radiative recombination lifetime will thus influence the dynamics of the RCLED. However, the change in lifetime is limited for practical cavities with an AlAs/GaAs DBR[5]. Besides this minor effect of practical planar cavities on the radiative recombination speed, the speed behavior of RCLEDs is similar to standard LEDs. Although the radiative recombination lifetime is slow, compared to stimulated emission, special techniques -background doping, the use of peaking current driver circuits or voltage drivers, smaller active regions- can be used to speed up the devices. The measured eye-diagram of a voltage-driven 980-nm RCLED (diameter is 30 μm) is shown in Fig. 5(b). Subnanosecond rise and fall times of the optical signals and communication with open eye diagrams at over 1Gb/s have been achieved[9]. Photon recycling increases the LED's response time to an electrical input signal. Photon recycling is thus beneficial for high efficiency applications but undesirable for high-speed communication devices.

4. STATE OF THE ART

510 and 650 nm emitting devices are commercially important for Plastic Optical Fibre (POF) based communication, which is now entering the infotainment market in automotive and consumer applications. POF represents the solution for low-cost networks. Moreover, due to their large diameter core, typically 0.5/1mm, POF systems require less demands on the tolerance of the fiber-optic coupler. POFs show a minimum absorption for wavelengths in the range of 510 nm. The most promising candidates to be used in this wavelength range are nitride based RCLEDs. Devices with InGaN/GaN multiple QWs and GaN/AlGaN DBRs, both MOCVD and MBE grown structures, are described. An MBE grown structure showed a 12-fold enhancement of external efficiency as compared with structures without resonant cavity[11]. The efficiency is mainly limited by the high In incorporation resulting in a lower internal efficiency.

A local absorption minimum of POFs is situated around 650 nm. In combination with the higher detector sensitivity, 650-nm devices offer a better compromise for POF-communication systems until now. Several standards are developed where a RCLED is used as source for POF based communication (Firewire or i.Link (IEEE1394b), Media Oriented System Transport (MOST)). Due to their visible wavelength, 650-nm RCLEDs can also serve a broad range of non-communication applications for which a high efficiency and directionality are important (scanners, optical mice, etc.). Like in standard LEDs, the GaAsP material system is increasingly substituted by the high quality AlGaInP. Due to the absorbing substrate (GaAs or Ge), the device is preferably top-emitting with a cavity sandwiched in between two DBR mirrors and an appropriate current injection design. A highly efficient top emitting RCLED grown by MOCVD operating at 650 nm and having a low forward voltage is reported[12]. A 300μmx300μm encapsulated device shows a wall-plug efficiency≈10.2%. The device, a λ-cavity with GaInP active layer enclosed by 2 $Al_xGa_{1-x}As$ DBRs, is ready for large scale production[13].

The target applications of 850-880 nm devices are (Fast)-Ethernet LAN data links (an 850-nm LED is the standard source for the approved standard for 100BASE-SX), remote control and infrared communication as regulated by *Infrared Data Association* (IrDA) (mainly because of the availability of low-cost Si-based detectors). The obvious material system for this wavelength range is GaAs, as its bandgap corresponds with this wavelength range. On the other hand this implies that the use of GaAs in the substrate, as part of the DBR, etc. will absorb this light. An 850 nm top emitting device, consisting of a λ-cavity sandwiched between 2 DBRs grown by MOCVD, shows an overall efficiency η_{ext} of 14.6%[14]. The top mirror is a 1.5 pair $Al_{0.15}Ga_{0.85}As$/ AlAs DBR, the bottom mirror a 20 pairs DBR. The decreased refractive index-contrast compared with a GaAs/AlAs DBR results in the need of a thicker DBR-stack. Current injection was optimized with a selectively oxidized current window with a diameter of 180μm. A 880 nm monolithic top emitting device with λ--cavity, a 20 pairs n-doped $Al_{0.2}Ga_{0.8}As$/ $Al_{0.9}Ga_{0.1}As$ bottom DBR and a 5-7 pairs top DBR, all grown by solid-source MBE is reported[15]. With an emission window of 80μm and an epoxy cap, η_{ext} is 16%.

980 nm infrared devices do not have a commercial killer application. Nevertheless, investigation on these devices has been carried out and is still going on as the GaAs/Al(Ga)As material system with InGaAs high quality strained QWs for active material makes these devices excellent proofs of principle. The design has been described above. Highly efficient bottom-emitting devices, grown by MOCVD are reported[10]. With a Au/(GaAs/AlAs)-DBR asymmetric λ-cavity, the metal layer both serving as electrical contact and as mirror, and three InGaAs strained QWs, the overall external efficiency of 80μm devices is up to 17%. When the diameter is larger, photon-recycling is more significant. An overall external efficiency up to 23% is obtained for large diameter (±1mm) RCLEDs, or a 1.4 enhancement. Leaky DBR modes, metal mirror absorption and a trapped guided mode are the main loss channels. According to section 3.1, a higher index-contrast DBR could result in higher efficiencies due to the suppressed leaky modes and decreased penetration depth. It can be achieved by laterally oxidizing the Al(Ga)As layers to obtain a high index-contrast AlOx/GaAs DBR mirror. There are some drawbacks however. This electrically isolating material necessitates advanced techniques like intra-cavity contacts. Moreover, the use of a high contrast DBR is less appreciated in combination with a metallic top mirror: for a high contrast DBR, the reflectivity of even a single pair is comparable with the gold mirror, resulting in detrimental metal absorption losses. The benefits of the use of a high index-contrast AlOx/GaAs DBR are thus limited to top emitting devices not using a metallic mirror. A laterally injected top emitting λ-cavity with a single 3.5 pair AlOx/GaAs bottom DBR, diameter 350μm, shows η_{ext} as high as 27%, encapsulated 28%[16].

The pre-eminently telecom-wavelengths are situated around 1300nm and 1500nm.The principal material system is InP. In addition to the broader intrinsic spectrum of long wavelength devices, the restrictions of the appropriate material systems (cf. Long wavelength VCSELs), limits the maximal efficiency of long wavelength devices. The problem lies in the low refractive index-contrast that can be realised with InP lattice matched alloys to form the DBR, resulting in large penetration depths. Highly efficient 1300 nm large diameter devices (2mm) with a peak quantum efficiency of 9% are reported[17], using a monolithic cavity grown by MOCVD. The electrically pumped device is bottom emitting, using an asymmetric Au/DBR InP λ-cavity with three 4.5 nm $InGa_{0.12}As_{0.56}P$ strained QWs . The low refractive index-contrast of the 5.5 pair $InGa_{0.23}As_{0.5}P$/InP DBR is the main drawback.

Research has an increasing interest in the development of GaAs based devices for long wavelength applications, i.e. active material compatible with GaAs. Next to the possibility of high index-contrast GaAs/AlAs Bragg mirror, this system is more temperature insensitive and cheaper. The use of Quantum Dots (QD) has been investigated in several

research groups. With self-assembled InAs-InGaAs QDs emitting at 1300 nm in a single mirror (Au) cavity, grown by solid-source MBE on a GaAs substrate, an external quantum efficiency of 1% at room temperature is obtained, limited by the low radiative efficiency of 13% of the QDs[18]. An MOCVD InP-based RCLED of diameter 80 μm emitting at 1550 nm with a 6.8% external quantum efficiency is cited. The device is bottom emitting, using an asymmetric Au/DBR(12 pairs $InGa_{0.38}As_{0.82}P$/InP) cavity. The active region consists of three 7.5 nm $In_{0.84}Ga_{0.16}As_{0.74}P_{0.26}$ QWs[18].

5. PHOTONIC CRYSTAL ASSISTED RCLED

The optical power in a planar RCLED is distributed over several modes. The resonance normal to the extraction interface, the Fabry-Perot mode, can be extracted. The optical power coupled to the leaky DBR modes, which are totally internally reflected at the semiconductor-air interface, and the optical power coupled to the laterally propagating modes (the guided modes), which are totally internally reflected at the DBR mirror, are lost (except through partial photon recycling by reabsorption). A solution to the loss of power in the unextractable guided modes can be found in a two-dimensional (2-D)-periodic wavelength-scaled grating or photonic crystal (PC) integrated into one or more of the interfaces of the resonant cavity. The planarity of the RCLED is abandoned, control on the in-plane dimensions is obtained.

Several design approaches can be distinguished. The periodic corrugation can provide a bandgap in the dispersion relation of the guided modes at the frequency of emission. Emission will then initially be prevented in the guided modes[20]. Eliminating the guided modes at the transition frequency, spontaneous emission can be enhanced to couple to the free space modes via the Fabry-Perot mode. Alternatively, the grating can be used for purely optical "photon recycling". The diffractive properties of the periodic grating can redirect the laterally propagating resonant guided mode to an extractable direction in the extraction cone. The 2-D periodic corrugation can be placed at the periphery of the LED's active area to extract the guided light reaching the edge of the device. In these devices, the Fabry-Perot mode is extracted in the central part of the light source where the layers are homogeneous, the guided mode leaves the semiconductor in the surrounding periodically corrugated region. Boroditsky *et al.* reported a 6-fold enhancement of the efficiency, but did not cite absolute efficiencies[21]. Rattier *et al.* predicts a supplementary extraction of 10% as worst case scenario[11]. Alternatively, the 2-D periodic corrugation can overlap with the active region. We call these devices Grating-Assisted Resonant-Cavity LEDs (GA-RCLEDs) (see Fig. 6(a)). The shallow grating with appropriate Bragg vectors integrated in one of the interfaces of the cavity will change the photon momentum of the light in the guided mode (with propagation constant larger than the vacuum wave vector). The propagation is broken and the light is diffracted towards the outside media. In the GA-RCLED, vertical and horizontal design issues are entangled. An ill designed GA-RCLED can affect existing extraction channels, resulting in a decrease of efficiency in comparison with gratingless RCLEDs. In view of this design issue, a periodic corrugation at the periphery of the active layer scores better. However, the GA-RCLED has more degrees of freedom concerning its dimensions than the device with a 2-D periodic corrugation at the periphery of the LED. For small injection diameters, the efficient use of available space decreases in case of the latter device. Due to the finite absorption length of the guided mode in the cavity, a limit is also posed on its maximal diameter (injection diameter <100 to 200 μm). The GA-RCLED has a maximal efficient use of available space independently on the diameter of the device. Moreover, diffraction of the guided mode starts at its origin, cancelling the upper limit on diameter size.

A bottom-emitting GA-RCLED has been designed and optimised for high extraction efficiency[21]. The device structure is sketched in Figure 6(a): the cavity has a periodic metallic top mirror and a bottom DBR-mirror. The central wavelength emitted by the GaAs based device is 980 nm. A rigorous plane wave expansion tool has been used to carry out the optimisation and design[22]. The simulated downwards TE-polarised internal net power flux per unit spatial frequency along k_x is plotted in Fig. 6(b). The internal net power flux per unit spatial frequency is as well simulated for its planar counterpart, described in section 3. The diffracted guided mode is clearly visible in the case of the GA-RCLED for $k_x \approx 0^o$.The simulated extraction efficiency is well over 40% when a spectral width of 20 nm is assumed.

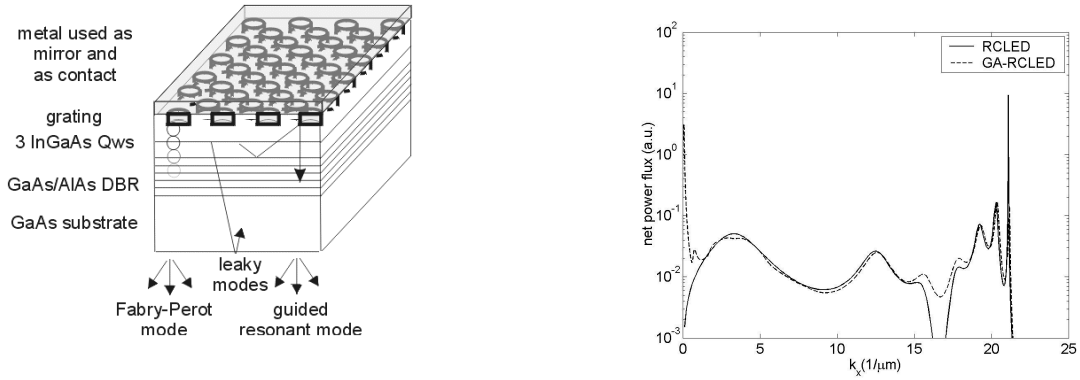

(a) (b)

Figure 6: (a) Sketch of GA-RCLED; (b) Simulated downwards TE-polarised internal net power flux per unit spatial frequency along k_x of RCLED and GA-RCLED.

A SEM picture of a cross-section of the device is shown in Fig. 7(a). The processing is described elsewhere[23,24] . The measured external efficiency and IV curve of a device with a diameter = 115μm are shown in Fig. 7(b). The device shows an external efficiency η_{ext} of 15.1%. The bottom-emitting device has a substrate of 500 μm. If we take into account an absorption of 22% after propagation through the 500 μm thick GaAs substrate (absorption coefficient ±5cm^{-1}) and the Fresnel reflections (±0.3 at normal incidence) the η_{ext} is as high as 27%. Its planar optimised RCLED counterpart shows an η_{ext} of 20%[3]. With an internal efficiency of 79%[24], the extraction efficiency is as high as 35%. Due to a detuned cavity (epistructure growth error and error on grating depth, both of several percents), the experimental results do not reach the numerically calculated or predicted efficiency of over 40%.

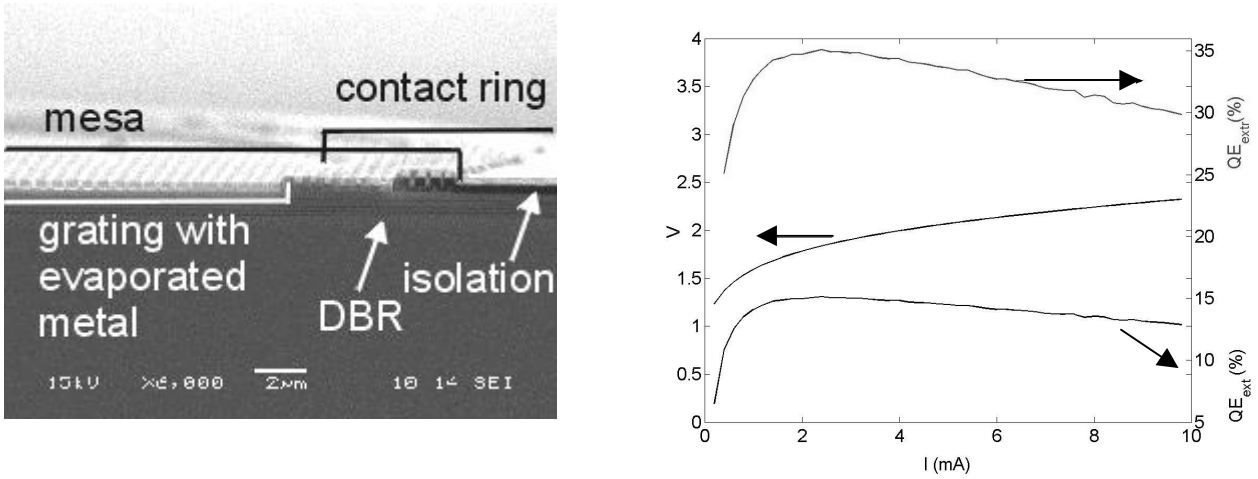

(a) (b)

Figure 7: (a) SEM picture of GA-RCLED; (b) Measured IV and QE (external and extraction) of GA-RCLED The period of the grating is 598 nm, the grating depth is ±50nm, diameter of etched holes is ±150nm.

6. CONCLUSION

Thorough investigation on RCLEDs has been carried out during the last decade. Efficiency, spectral purity, modulation behavior, etc. have been analysed theoretically and experimentally. A broad range of wavelengths are available due to extrapolation of the principle to different material systems. Moreover, this high-efficiency light-emitter is no longer just an object of research. It has been launched commercially in the POF communication market and non-communication

applications (scanners etc.). The key merits of the RCLED that make the device attractive for these applications can be found in its planar, single side extraction appearance, allowing for 1D and 2D dense arrays in combination with both a high efficiency and high radiance or brightness. Fabrication of a RCLED is similar to the fabrication of conventional planar LEDs: straightforward and at low cost. RCLEDs do not have a threshold current and therefore they can outperform the high radiant VCSEL in situations where a high efficiency is needed at a low power operation point. This can be the case in high density array applications, which are the target applications of RCLEDs: massively parallel optical data communication, sensors, printers etc.

Investigation is now focussed on new material systems, similar as the research of standard LEDs, and on adavanced techniques to enhance even further the efficiency and radiance of the device. Photonic crystals are used to control the in-plane dimensions of the planar device. The use of these multi-dimensional periodic corrugations do influence strongly the optical mode density resulting in alteration of emission profile and/or emitted power. Extraction enhancements of 60% are experimentally obtained with a GA-RCLED.

In conclusion it is clear that the RCLED can serve a broad range of low cost, high volume applications, both communication and non-communication, and this for a broad range of wavelengths. The RCLED can be a favorable choice in comparison to VCSELs and most high efficiency LEDs when: a relatively high radiance is needed, modulation bandwidth of 1GHz suffices and when the incoherent nature of the source is not a problem or is even an asset. In particular dense array applications do profit from the combination of properties of the RCLED.

ACKNOWLEDGMENTS

Peter Bienstman ackownledges the support from the Flemish Fund for Scientific Research (FWO - Vlaanderen) for a postdoctoral fellowship.

REFERENCES

1. E. F. Schubert, Y.-H. Wang, A. Y. Cho, L.-W. Tu and G. J. Zydzik, "Resonant Cavity light-emitting Diode", *Appl. Phys. Lett.*, **60(8),** pp. 921-923, 1992.
2. H. Benisty, R. Stanley and M. Mayer, "Method of source terms for dipole emission modification in modes of arbitrary planar structures", *J. Opt. Soc. Am. A*, **15(5),** pp. 1192-1201, 1998.
3. D. Delbeke, R. Bockstaele, P. Bienstman, R. Baets and H. Benisty, "High-Efficiency Semiconductor Resonant-Cavity Light-Emitting Diodes: a review", *Journ. Select. Topics Quant. Electr.*, **8(2)**, pp. 189-206, 2002.
4. P. Bienstman and R. Baets, "The RC2LED: an novel Resonant-Cavity LED design using a symmetric resonant cavity in the outcoupling reflector", *Journ. Quant. Electr.*, **36(6)**, pp. 669-673, 2000.
5. I. Abram, I. Robert and R. Kuszelewicz, "Spontaneous Emmission Control in Semiconductor Microcavities with Metallic or Bragg Mirrors", *Journ. Quant. Electr.*, **34(1)**, pp. 71-76, 1998.
6. G. Bourdon, I. Robert, R. Adams, K. Nelep, I. Sagnes, J.M. Moison and I. Abram, "Room temperature enhancement and inhibition of spontaneous emission in semiconductor microcavities", *Appl. Phys. Lett.,* **77(9),** pp. 1345-1347, 2000.
7. J.M. Gérard and B. Gayral, "Strong Purcell effect for InAs quantum boxes in three-dimensional solid-state microcavities", *J. Lightwave Techn.*,**17(11)**, pp. 2089-2095, 1999.
8. E. F. Schubert, N. E. J. Hunt, R. J. Malik, M. Micovic and D. L. Miller, "Temperature and Modulation Characteristics of Resonant-Cavity light-emitting Diodes", *Journ. of Lightwave Techn.*, **14(7)**, pp. 1721-1729, 1996.
9. R. Bockstaele, T. Coosemans, C. Sys, L. Vanwassenhove, A. Van Hove, B. Dhoedt, I. Moerman, P. Van Daele, R.G. Baets,R. Annen, H. Melchior, J. Hall, P.L. Heremans, M. Brunfaut and J. Van Campenhout, "Realization and characterization of 8X8 resonant cavity LED arrays mounted onto CMOS drivers for POF-based interchip interconnections", *Journ. Select. Topics Quant. Electr.*, **5(2)**, pp. 224 -235, 1999.
10. H. De Neve, J. Blondelle, P. Van Daele, P. Demeester, R. Baets and G. Borghs, "Recycling of Guided Mode Light Emission in Planar Micro-cavity Light Emitting Diodes", *Appl. Phys.Lett.*, **70(7)**, pp. 799-801, 1997.
11. F.B. Naranjo, S. Fernandez, M.A. Sanchez-Garcia, F. Calle and E. Calleja, "Resonant-Cavity InGaN multiple-quantum-well green ligth emitting diode grown by MBE", *Appl. Phys. Lett.*, **80(12),** pp. 2198-2200, 2002.
12. R. Wirth, C. Karnutsch, S. Kugler and K. Streubel, "High efficiency resonant cavity LEDs emitting at 650 nm", *Photon. Technol. Lett.*, **13(5)**, pp. 421-423, 2001.

13. R. Wirth, W. Huber, C. Karnutsch and K. Streubel, “Resonators provide LEDs with laser-like performance”, *Compound Semiconductor,* 01/2002.
14. R. Bockstaele, J. Derluyn, C. Sys, S. Verstuyft, I. Moerman, P. Van Daele and R. Baets, “Realisation of highly efficient 850nm top emitting resonant-cavity light-emitting diodes”, *Electr. Lett.*, **35(18),** pp. 1564-1565, 1999.
15. P. Sipila, M. Saarinen,V. Vilokkinen, S. Orsila,P. Melanen, P. Savolainen, M. Toivonen, M. Dumitrescu and M. Pessa, “Resonant cavity LEDs at 655 and 880 nm wavelengths”, in *Light-Emitting Diodes : Research, Manufacturing, and Applications IV*, H. Walter Yao, Ian T. Ferguson and E. Fred Schubert, eds., Proc. SPIE 3938, pp. 82-89, 2000.
16. M. Rattier, H. Benisty, R.P. Stanley, J.-F. Carlin, R. Houdré, U. Oesterle, C.J.M. Smith, C. Weisbuch and T. F. Krauss, “Toward Ultrahigh-Efficiency Aluminium Oxide Microcavity Light-Emitting Diodes: Guided Mode Extraction by Photonic Crystals”, *Journ. Select. Topics Quant. Electr.*, **8(2)**, pp. 238 -247, 2002.
17. B. Depreter, I. Moerman, R. Baets, P. Van Daele and P. Demeester, “InP based 1300 nm microcavity LEDs with 9% quantum efficiency”, *Electr. Lett.*, **36(15)**, pp. 1303-1304, 2000.
18. A. Fiore, U. Oesterle, R.P.Stanley, R. Houdre, F. Lelarge, M.Ilegems, P. Borri, W. Langbein, D.Birkedal, J.M.Hvam, M. Cantoni and F. Bobard, “Structural and electrooptical characteristics of quantum dots emitting at 1.3 μm on gallium arsenide”, *IEEE Journ. Quant. Electr.*, **37(8**), pp. 1050-1058, 2001.
19. B. Depreter, S. Verstuyft, I. Moerman, R. Baets and P. Van Daele, “InP-based microcavity light emitting diodes emitting at 1.3μm and 1.55μm”, *Proc. of the 11th International Conference on InP and related materials (IPRM),*Davos, Switserland 16-20 may, 1999, pp. 227-230 , 1999.
20. M.G. Salt, P. Andrew and W.L. Barnes, “Microcavities, texture symmetry, and photonic bandgaps,” *J. Opt. Soc. Amer. B*, **18(20)**, pp. 240-243, 2001.
21. M. Boroditsky, T.F. Krauss, R. Coccioli, R. Vrijen, R. Bhat and E. Yablonovitch,, “Light extraction from optically pumped light-emitting diode by thin-slab photonic crystal”, *Appl. Phys. Lett.*, **75(8),** pp. 1036-1038, 1999.
22. D. Delbeke, P. Bienstman, R. Bockstaele and R. Baets, “Rigorous Electromagnetic Analysis of Dipole Emission in Periodically Corrugated Layers: the Grating-Assisted Resonant-Cavity Light-Emitting Diode,” *J. Opt. Soc. Am. A*, **11(5)**, 871-880, 2002.
23. D. Delbeke, C. Sys, I. Moerman, P. Van Caele and R. Baets, “ Electrically Pumped Grating-Assisted Resonant-Cavity Light-Emitting Diodes”, in *Proc. SPIE Light Emitting Diodes: Research, Manufacturing and Applications VI*, **4641**, pp. 42-49, 2002.
24. K. Ghawana, D. Delbeke, I. Christiaens, S. Verstuyft and R. Baets, “Grating-Assisted Resonant-Cavity LEDs: towards thin film devices for heterogeneous integration”, in *Optoelectronic devices and heterogenous integration, Proc. SPIE*, **4947**, Brugge, Belgium, 2002.